Measurement of C^{3+} dielectronic recombination in a known external field

A. R. Young,* L. D. Gardner, D. W. Savin, G. P. Lafyatis,† A. Chutjian,‡ S. Bliman,§ and J. L. Kohl
Harvard-Smithsonian Center for Astrophysics, 60 Garden Street, Cambridge, Massachusetts 02138
(Received 10 August 1993)

An experiment to measure the dielectronic recombination of C^{3+} in a known external electric field is described. The measured value differs from results of calculations which do not include the effects of field enhancement, and is larger than but marginally in agreement with predictions of theoretical methods that include the effects of the external field.

PACS number(s): 34.80.Kw, 34.80.Dp, 35.80.+s

I. INTRODUCTION

In this paper, we present a measurement of dielectronic recombination (DR) in a known external electric field. It is believed that external fields significantly enhance the DR rate coefficient under certain circumstances [1], suggesting the need for a body of experimental data in which the DR rate coefficient is measured for several different species and several well-specified values of the external field strength.

The interpretation of experimental data from beam experiments and plasmas is complicated by the difficulties in directly measuring and controlling the electric fields present in the ion rest frame. The status of experiments that measure DR is reviewed in Ref. [2]. In all but one case [3,4], the fields were not directly determined.

For the present work, the electric fields in the ion rest frame were controlled through an inclined-beams geometry. A magnetic field, directed along the electron beam axis, transforms into a motional electric field in the ion rest frame. The ion velocity and the magnetic field vectors can be measured; thus the magnitude and orientation of the electric field can be determined.

The DR process studied in this work involves the $1s^2 2s\ {}^2S_{\frac{1}{2}} \leftrightarrow 1s^2 2p\ {}^2P^o_{\frac{3}{2},\frac{1}{2}}$ transition in a C^{3+} ionic core (a $\Delta N = 0$ transition, where N is the principal quantum number of the active core electron). Ignoring for the moment the possible effect of an external electric field, the subject process can be represented by the following equation:

$$C^{3+}(1s^2 2s) + e \leftrightarrow C^{2+}(1s^2 2p, nl)^{**} \rightarrow C^{2+}(1s^2 2s, nl)^{*} + h\nu(\lambda \simeq 155\ \text{nm}), \quad (1)$$

where n is the principal quantum number and l the angular momentum quantum number of the captured electron. For incident electron energies just below the threshold for the $2s$-$2p$ transition, the electrons are captured predominantly into high-n levels.

The choice of C^{3+} is motivated by several different factors. The enhancement mechanism is thought to be largest when DR proceeds primarily through doubly-excited states with the captured electron in a high-n level, since such levels are the most sensitive to the presence of fields [2]. This is often the case for DR in low to moderate Z ions and DR involving $\Delta N = 0$ transitions. Both conditions apply in the case of C^{3+} studied here. In addition, radiation from C^{3+} is a prominent feature of many astrophysical plasmas. Since DR is often the dominant recombination mechanism for C^{3+} in these plasmas, field enhancement may play some role in the interpretation of the measured UV spectra.

II. EXPERIMENTAL APPROACH

Relatively large photon and charge-reduced ion backgrounds present in beam experiments can be efficiently overcome by measuring, in delayed coincidence, recombined ions and photons emitted at wavelengths appropriate for DR events. The simultaneous emission of a stabilizing photon and a recombined ion serves to tag the DR process. A detailed description of an implementation of this method, first proposed for the measurement of DR by Lafyatis and Kohl [5], is found elsewhere [6]. It has also been used by other experimenters [7,8] to measure DR in Mg^+ and Ca^+. A schematic of the experimental apparatus used in this work is found in Fig. 1.

There are several aspects of this experiment which distinguish it from other DR coincidence experiments. A unique photon collection system, composed of a deep spherical mirror placed within 1 cm of the ion beam,

*Present address: Physics Department–Jadwin Hall, Princeton University, Princeton, NJ 08544.
†Present address: L.S.A.I., Université Paris Sud, 91405 Orsay, France.
‡Present address: Jet Propulsion Laboratory 183-601, 4800 Oak Grove Drive, Pasadena, CA 91109.
§Present address: Department of Physics, Ohio State University, 174 W. 18th Ave., Columbus, OH 43210.

intercepts a solid angle of π steradians at the beams-intersection volume. This results in a relatively large photon detection efficiency. The mirror also has imaging properties that limit the photon backgrounds resulting from photons emitted outside the beams' intersection region [9,10]. The detection of recombined ions, as opposed to neutral atoms, permits a straightforward, precise determination of the absolute recombined ion detection efficiency as well.

The DR rate coefficient can be expressed as a function of experimentally determined quantities as follows:

$$\langle v\sigma_{\rm DR}\rangle_E = \int \sigma_{\rm DR}(E)v_r(E)P(E)dE = \frac{S_{\rm DR}}{\xi \int N_I(x,y,z)n_e(x,y,z)I(x,y,z)\eta(x,y,z,\tau)dxdydz}. \quad (2)$$

The rate coefficient is defined as an integral over the electron's energy, involving $\sigma_{\rm DR}(E)$, the DR cross section as a function of energy, $v_r(E)$, the relative velocity between the ions and electrons, and $P(E)$, the probability an electron will have an energy between E and $E+dE$. On the right-hand side, $S_{\rm DR}$ is the coincidence signal due to DR, ξ is the fraction of the beam in the ground state of C^{3+}, N_I and n_e are the the ion and electron densities, v_r is the relative velocity, and I and η are the detection efficiencies for recombined ions and the photons, respectively. For this work, we take $\eta(x,y,z,\tau) = \epsilon(x,y,z,\tau)Y_\Omega(x,y,z)$, where $\epsilon(x,y,z,\tau)$ is the detection efficiency for the photons (τ is the lifetime of the radiative process), and $Y_\Omega(x,y,z)$ is the angular anisotropy factor for the emitted photons. The integral in the denominator of Eq. (2) is called the overlap-efficiency (OE) integral. An experimental determination of the rate coefficient consists of evaluating each of the elements of the right-hand side of this equation. For a meaningful comparison to theoretical predictions of the cross section, $v_r(E)$, $P(E)$, and the electric fields in the experimental geometry must be specified as well.

The experiment is run with the electron beam periodically switched between an on-resonance value where the DR rate coefficient is to evaluated, and an off-resonance value where the DR rate is expected to be negligible. The DR signal is extracted as a difference between the on-resonance and the off-resonance coincidence data. For the present work, the off-resonance coincidence trace was obtained with the electron beam switched off. The ideal tactic is to switch the energy from an on-resonance setting to one above the threshold for excitation where DR is not expected to occur. This will be done in the future in order to ensure that any electron generated backgrounds are subtracted (although there was no evidence for these backgrounds in preliminary measurements of DR performed in this laboratory [6]).

The delay interval corresponding to the coincidence window was determined by detecting delayed photon/ion coincidences from charge transfer (CT) of C^{3+} on H_2. This process results in an excited state of C^{2+}, which then radiates a detectable photon. The coincidence signal due to CT into excited states can be made quite large by removing a quartz filter and increasing the H_2 pressure in the interaction region (see Fig. 1). With the existing apparatus, spectra such as that depicted in the bottom of Fig. 2 can be obtained in a few hundred seconds. The position and width of the coincidence window are in accord with estimates based on the timing properties of the electronics and the experimental geometry. A careful analysis of the coincidence signal due to CT has been

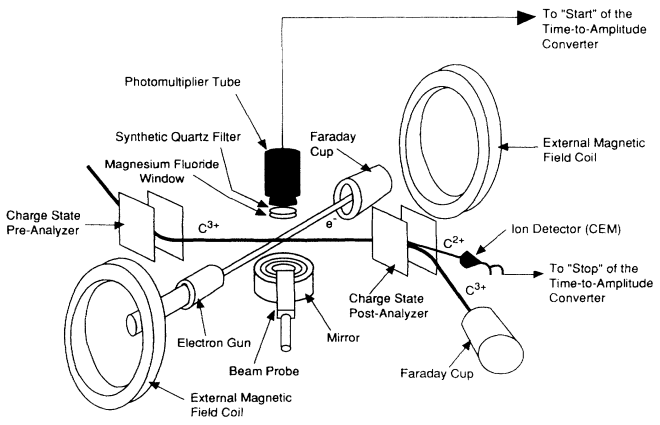

FIG. 1. Schematic diagram of the experimental apparatus.

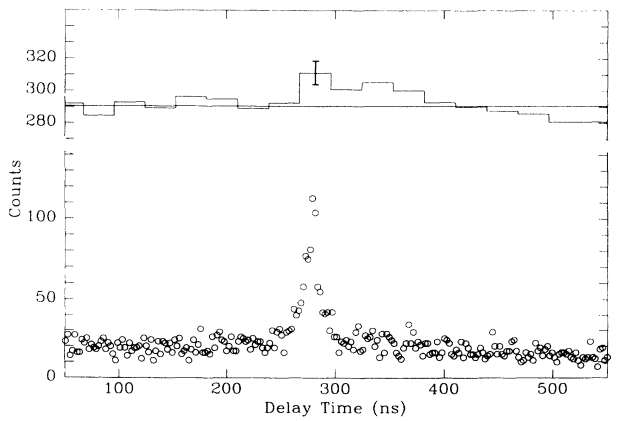

FIG. 2. The sum of all the DR coincidence data (top) is depicted versus the delay time between detection of a photon and of a C^{2+} ion. The DR data are summed in 28 ns bins. A linear fit to the residual accidental background is shown as a straight line. Charge-transfer data used to determine the coincidence window are shown in the bottom plot.

made as well [9]. The measured signal is consistent with the measurements of CT into excited states performed by Ćirić *et al.* [11].

A. Particle densities and ion-detection efficiency

The technique used to determine the particle densities was to measure the current density profile for each beam in a plane passing through the center of the interaction volume [12]. Possible contaminants of the ion beam (O^{4+} and a population of metastable states of C^{3+}) are considered elsewhere and found to be negligible [9].

The recombined ion-detection efficiency can be expressed as the product of two factors: $I(x,y,z) = P(x,y,z)\Theta(x,y,z)$, where $P(x,y,z)$ is the probability that an ion which recombined at (x,y,z) will reach the channel electron multiplier (CEM), and $\Theta(x,y,z)$ is the counting efficiency for the recombined ions in the CEM. The first factor, $P(x,y,z)$, can be determined by comparing the current in the primary ion beam measured in the interaction region (using the automated beam probe) with the current in the CEM. The ion counting efficiency, $\Theta(x,y,z)$, was determined from a measurement of C^{2+} due to charge transfer of C^{3+} with H_2. The ratio of the C^{2+} current (at an H_2 pressure of 4.5×10^{-7} torr) to the C^{2+} particle count rate (with the H_2 pressure reduced by a known factor) provided the ion counting efficiency. A typical measured value for $\Theta(x,y,z)$ was 0.53 ± 0.03, where the principal contribution to the uncertainty was the stability of the ion source.

Measurements of the efficiency taken when the DR data were obtained indicate that the CEM efficiency fell over the course of the day. The efficiency and ion background data provided sufficient information to put limits on the CEM efficiency variation, which was $\pm15\%$ of the mean efficiency.

B. Photon-detection efficiency

The photon-detection efficiency for any point in the interaction volume is a product of several factors. The mirror, used to concentrate the photons from the interaction region onto the photomulltiplier tube (PMT), has rough imaging properties. This manifests itself as a photon-detection efficiency that is a function of position in the interaction volume. Because the imaging aberrations are large, precise models of the photon system's detection efficiency must be made (also taking into account the variation in the response of the PMT across its face). In addition to this position dependent factor, the overall photon-detection efficiency is proportional to the reflectance of the mirror, the transmittance of two wire grids, the magnesium fluoride window, the quartz filter, and the (average) counting efficiency of the PMT. These latter factors can be collected into a single, position independent quantity, ε_γ. This constant was determined by normalizing a measurement of the C^{3+} electron-impact excitation (EIE) rate coefficient near threshold to theoretical values for this cross section (this is discussed further in Sec. III). In addition to these considerations, the effect of the lifetime of the radiating ions must be considered as well. This is treated elsewhere, and is shown to be a negligible effect for ions undergoing DR [9].

C. Electric field in the ion rest frame

The magnitude and direction of the electric field in the ion rest frame is determined primarily by the magnetic field applied in the laboratory. The other principal contributors to the electric field are the space charge in each of the beams. The fringing fields of the analyzers, the earth's magnetic field, and residual magnetic fields from the ion source make small additions as well. The net magnetic field in the laboratory will result in an electric field in the ion rest frame with a value of $\vec{E} = \vec{v_I}\times\vec{B}$, where $\vec{v_I}$ is the ion velocity, and $\vec{B}$ is the magnetic field. The direction of the ion beam is constrained by a series of apertures in the experimental apparatus, and the magnitude of the ion velocity is determined by time-of-flight methods. The magnetic fields are measured with a Hall effect magnetic field meter.

The fields due to the distribution of charge in the ion beam are smaller than 0.1 $\mathrm{V\,cm^{-1}}$. The electrons produce a field which is smaller than 1.3 $\mathrm{V\,cm^{-1}}$ (a worst case estimate). Fringing fields due to the analyzers were investigated and found to be smaller than 0.1 $\mathrm{V\,cm^{-1}}$. The total electric field is taken to be the vector sum of the radial field due to the space charge of the electrons and the motional electric field. We treat the radial field as an uncertainty in the value of the electric field. There are also small contributions to the uncertainty of the field strength due to uncertainties in the ion beam's velocity. All the uncertainties added in quadrature result in an uncertainty of ±1.6 $\mathrm{V\,cm^{-1}}$.

A complete theoretical modeling of the experimentally determined rate coefficient must also include the electric fields along the ion's path between the collision volume and the ion detector [13,14]. Of particular importance are the relatively strong fields in the final charge-state analyzer. The analyzer field ionizes some of the recombined ions, limiting the measured rate coefficient.

III. EXCITATION RESULTS AND ANALYSIS

The EIE rate coefficient for the $1s^22s\,^2S$ to $1s^22p\,^2P^o$ transition in C^{3+} was measured before and after the DR experiments. Near-threshold EIE data taken prior to and after the DR experiment provided the absolute scale for the ion rest frame energy of the electrons. Also, the energy distribution of the electrons and the photon detection efficiency were derived from the EIE data taken before and after the DR experiment. The procedure was similar to that described in previous papers [6].

The rate coefficient data, normalized to the theory, are depicted in Fig. 3 (error bars represent the statistical uncertainty at the 90% confidence level). The lowest-energy point overlapped with zero, largely confirming the absence of any significant spurious signal associated with

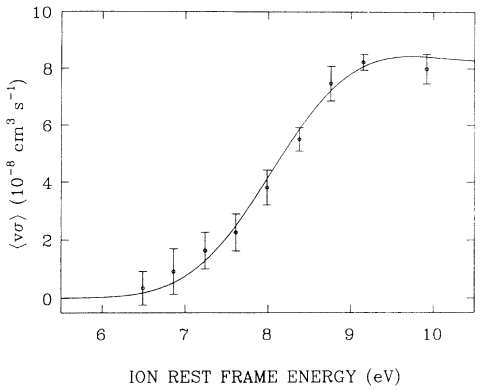

FIG. 3. The EIE rate coefficient near threshold for the $1s^2 2s\,^2S$ to $1s^2 2p\,^2P^o$ transition in C^{3+}. The solid curve is the best fit of the experimental data to theory [15]. The error bars on the data are statistical uncertainty at the 90% confidence level.

beam-modulated backgrounds.

Normalization to theory involves the convolution of the theoretical cross section with the experimental energy distribution. The analytical expression for the cross section versus energy is taken from the two state close-coupling work of Gau and Henry [15]. The free parameters were varied to determine the best fit and to estimate the range of values that are consistent with the data. The full width at half maximum (FWHM) of the electron beam energy distribution in the ion rest frame was found to be 1.80 ± 0.47 eV, and the offset potential was similarly found to be 1.71 ± 0.26 V.

The relatively large width of the electron energy distribution is consistent with a more typical value of 0.5 eV for the electrons prior to their exiting the electron gun. The magnetic fields at the mouth of the gun are seen to have sizable gradients due to the presence of μ metal around the electron gun. These gradients can increase the size of the transverse velocity components, thereby increasing the spread in the ion rest frame energy. Electron trajectories through a model field geometry were calculated to verify that the observed energy spreads were reasonable. The scale factor will be discussed in Sec. IV.

IV. DR RESULTS AND ANALYSIS

The signal due to DR in C^{3+} is obtained by subtracting a coincidence trace with the electron beam off from a coincidence trace with the electron beam energy centered on the expected DR peak. The DR signal is extracted from the difference spectrum by fitting the background outside the coincidence window with a least-squares fit and subtracting this from the DR coincidence peak.

Typical operating conditions are shown in Table I. The current in the magnetic coils, which were used to apply fields in the interaction region, varied by less than 1% for all measurements. The backgrounds and currents were monitored for each run. These monitor data were used to evaluate each run and to compute average background rates.

TABLE I. Representative operating conditions for the DR experiment.

Pressure (ionization gauge reading)	3×10^{-10} torr
Electron beam current	50 μA
Ion beam current	0.30 μA
Ion background rate	2.3×10^5 s^{-1}
Photon Background	
due to electron beam	110 s^{-1}
due to ion beam	50 s^{-1}
dark rate	$\leq$ 1 s^{-1}
DR coincidence count rate	0.06 s^{-1}
Coincidence window width	28 ns
Average run time	10^3 s

The DR measurement is the result of nine runs. The value for the final rate coefficient was computed using an average of the nine measured rate coefficients weighted so that the most reliable data have the largest weight [16]. The sum of all the difference spectra is shown in the top of Fig. 2. These data are presented as a histogram with 28 ns wide bins. The DR coincidence window is indicated by the error bar. Although the final result was derived from rate coefficients obtained for each run separately, this sum exhibits several important features of the coincidence data. Outside of the coincidence window, the trace is flat. This is consistent with the idea that this background is due to accidental coincidences. This background was determined with a least-squares fit to the data outside the coincidence window.

Another satisfying feature of the data is that the χ^2 per degree of freedom for the deviations of the background data from the line generated by the least-squares fit is 1.04. Since there is a 33% chance of randomly observing a larger value of χ^2, this indicates a reasonable statistical distribution around the line. A check for large scale structure in the background is to add a quadratic term to the fit. Adding this term reduces the signal computed from the data by 32%. This change is on the order of the statistical uncertainty of the signal ($\pm$30% at the 68% confidence level), and indicates that this does not produce a statistically significant change in the DR measurement. Hence, the background is assumed to be flat, consistent with an expectation of a background due only to accidental coincidences.

The final result measured for the DR rate coefficient at a peak ion rest frame energy of 8.01 ± 0.20 eV is

TABLE II. Sources of uncertainty for the DR measurement.

Source of uncertainty	Uncertainty (%)
Overlap-integral normalization	21
Uncertainty in PMT uniformity	19
Variation in the overlap integrals during a run	11
Variation in CEM efficiency	15
Absolute ion-detection efficiency	4
Statistics (1σ)	30
Sum in quadrature (1σ)	45

$(3.6 \pm 1.6) \times 10^{-10}$ $cm^3 s^{-1}$ (at the 68% confidence level). The sources of the uncertainties quoted above are displayed in Table II. This measurement is dominated by statistical uncertainties (±30%). The absolute scale for the DR measurement is partially determined by normalizing the EIE energy-averaged cross section to theory. The scale factor ε_γ, deduced by the fitting procedure discussed previously, is $(6.9 \pm 1.0) \times 10^{-3}$. The uncertainty in the normalization procedure is the sum, in quadrature, of the (statistical) uncertainty in the scale factor, the OE integral variability [see Eq. (2)], and a ±15% uncertainty due to the possible presence of a low-energy tail in the electron energy distribution [17]. The total is ±21%. The uncertainty in the uniformity of the PMT response introduces a ±19% uncertainty into this normalization procedure.

Photon anisotropy factors, as they pertain to this inclined-beams geometry, have been discussed elsewhere [9,12]. In this work, we take $Y_\Omega = 1$.

V. COMPARISON TO THEORY

The measured rate coefficient can now be compared with theory. The energy distribution, derived from the excitation data, and the electric fields in the interaction region and post analyzer serve to unambiguously determine the conditions under which the DR rate coefficient was measured. In the present comparison to theory, the cutoff n of the captured electron due to field ionization was calculated, using the usual hydrogenic formula [18], to be $n_{max} = 43$. Table III lists the DR rate coefficient measured in this work and the predicted DR rate coefficients for no external electric field and for an external field strength of 12 $V cm^{-1}$.

There are several points to note concerning the comparison. The first is that this measurement differs from the theoretical zero field rate coefficients [19–21]. The field effect is required for theoretical calculations to approach agreement with our measurement. It should be noted that the uncertainty in the spread of the electron energy translates into a significant uncertainty in the predicted rate coefficient, but does not alter this conclusion.

The second point is that the measured value of the field-enhanced rate coefficient is a factor of 2.8 larger than that predicted by LaGattuta [22], and a factor of 1.8 larger than that predicted by Griffin *et al.* [20,21]. At present, our experimental uncertainties may account for the difference between the predicted and measured rates. The work of Dittner [23] also indicated a rate coefficient that is larger (by a factor of 1.5) than rate coefficients predicted by Griffin *et al.* [21]. On the other hand, the recent work of Andersen *et al.* [24] may be in better agreement with theory. It should be noted that the fields were not precisely known in either of the latter experiments.

The rate coefficients calculated by Griffin are generally larger than those of LaGattuta and McLaughlin and Hahn. One of the principal differences between the two calculations is that the work of Griffin includes fine structure interactions (it is an intermediate coupling calculation). Also, field enhancement appears to be smaller when intermediate coupling calculations are performed.

TABLE III. Comparison of DR rate coefficient measurement to theoretical predictions. F denotes the external field strength. Experimental uncertainties are absolute, and at the 68% confidence level.

Source	Rate coefficient (10^{-10} $cm^3 s^{-1}$)	
	$F = 0$ $V cm^{-1}$	$F = 12$ $V cm^{-1}$
Present work		3.6 ± 1.6
McLaughlin and Hahn [19]	0.5	
LaGattuta [22]		1.3
Griffin *et al.* [20,21]	0.7	2.0

We note here that the hydrogenic formula, used to determine the cutoff n due to field ionization in the final charge-state analyzer, is an approximate formula. A more detailed model of field ionization may be required to accurately predict the measured DR rate for high precision measurements. A final point is that neither of these calculations takes into account the field rotation effects [13] on the measured recombination rate coefficient or the possibility of overlapping-interacting resonances [25]. Both effects tend to push the experimentally determined rates out of agreement with theory, but are expected to be small and should not result in a dramatic change to the conclusions drawn from the experiment.

VI. SUMMARY

The measured DR rate coefficient of $(3.6 \pm 1.6) \times 10^{-10}$ $cm^3 s^{-1}$ (68% confidence error bars) differs from calculations that do not include enhancement by the external field. The present result is consistent with another experiment [23] that indicates larger field-enhanced rates than are predicted theoretically. Clearly, additional data are required to discriminate between various theoretical treatments of field enhancement, fine structure effects, and the effect of fields along the path of the recombined ions.

ACKNOWLEDGMENTS

The authors gratefully acknowledge stimulating conversations with W. H. Parkinson, G. Victor, and D. C. Griffin. We also acknowledge the skilled technical assistance of F. P. Rivera and D. Smith and the programming assistance of G. M. Gardner. This work was supported in part by NASA Grant No. NAGW-1687 to Harvard University and and by a Scholarly Studies grant from the Smithsonian Institution. Preliminary work leading to this measurement was supported by the Office of Basic Energy Science, Chemical Sciences Division, of the U.S. Department of Energy under Grant No. DE-FG02-86ER13634 to the Smithsonian Institution.

[1] V. L. Jacobs, J. Davis, and P. C. Kepple, Phys. Rev. Lett. **37**, 1390 (1976). An earlier paper by Burgess and Summers suggested an enhancement mechanism due to electron collisions; see A. Burgess and H. P. Summers, Astron. J. **157**, 1007 (1969).

[2] *Recombination in Atomic Ions*, edited by W. G. Graham, W. Fritsch, Y. Hahn, and J. A. Tanis (Plenum Press, New York, 1992).

[3] A. Müller, D. S. Belić, B. D. DePaola, N. Djurić, G. H. Dunn, D. W. Mueller, and C. Timmer, Phys. Rev. Lett. **56**, 127 (1986).

[4] A. Müller, D. S. Belić, B. D. DePaola, N. Djurić, G. H. Dunn, D. W. Mueller, and C. Timmer, Phys. Rev. A **36**, 599 (1987).

[5] G. P. Lafyatis and J. L. Kohl, Bull. Am. Phys. Soc. **24**, 1181 (1979).

[6] L. D. Gardner, J. L. Kohl, G. P. Lafyatis, A. R. Young, and A. Chutjian, Rev. Sci. Instrum. **57**, 2254 (1986).

[7] D. S. Belić, G. H. Dunn, T. J. Morgan, D. W. Mueller, and C. Timmer, Phys. Rev. Lett. **50**, 339 (1983).

[8] J. F. Williams, Phys. Rev. A **29**, 2936 (1984).

[9] A. R. Young, Ph.D. thesis, Harvard University, 1990 (unpublished).

[10] A. R. Young, L. D. Gardner, D. W. Savin, D. B. Reisenfeld, and J. L. Kohl (unpublished).

[11] D. Ćirić, A. Brazuk, D. Dijkkamp, F. J. de Heer, and H. Winter, J. Phys. B **18**, 3629 (1985). Related experimental work is discussed in P. G. Yan, R. Van der Woude, D. Dijkamp, and F. J. De Heer, Phys. Scr. **T3**, 120 (1983); and in F. G. Wilkie, R. W. McCullough, and H. B. Gilbody, J. Phys. B **19**, 239 (1986).

[12] G. P. Lafyatis, J. L. Kohl, and L. D. Gardner, Rev. Sci. Instrum. **58**, 383 (1987).

[13] K. LaGattuta, I. Nasser, and Y. Hahn, Phys. Rev. A **33**, 2782 (1985).

[14] C. Bottcher, D. C. Griffin, and M. S. Pindzola, Phys. Rev. A **34**, 860 (1986).

[15] J. N. Gau and R. J. W. Henry, Phys. Rev. A **16**, 986 (1977).

[16] William R. Leo, *Techniques for Nuclear and Particle Physics Experiments* (Springer-Verlag, Berlin, 1987), p. 90.

[17] Retarded potential analysis of the electron beam indicated the presence of a low-energy tail containing 15% of the integrated beam current. Because of the difficulties in interpreting retarded potential analysis data, we chose to treat the presence of this tail as an additional uncertainty in the magnitude of the overlap. Additional information on the retarded potential analysis data can be found in Ref. (9).

[18] F. Brouillard, in *Atomic and Molecular Processes in Controlled Thermonuclear Fusion*, edited by C. J. Joachain and D. E. Post (Plenum, New York, 1983).

[19] D. J. McLaughlin and Y. Hahn, Phys. Rev. A **27**, 1389 (1983).

[20] D. C. Griffin (private communication).

[21] D. C. Griffin, M. S. Pindzola, and C. Bottcher, Phys. Rev. A **33**, 3124 (1985).

[22] K. J. LaGattuta, J. Phys. B **18**, L467 (1985).

[23] P. F. Dittner, Phys. Scr. **T22**, 65 (1988).

[24] L. H. Andersen, J. Bolko, and P. Kvistgaard, Phys. Rev. A **41**, 1293 (1990).

[25] D. A. Harmin, Phys. Rev. Lett. **57**, 1570 (1987).